POLITECNICO DI TORINO
Repository ISTITUZIONALE

Sterics and Hydrogen Bonding Control Stereochemistry and Self-Sorting in BINOL-Based Assemblies

Original
Sterics and Hydrogen Bonding Control Stereochemistry and Self-Sorting in BINOL-Based Assemblies / Zou, Y.-Q., Zhang, D., Ronson, T.K., Tarzia, A., Lu, Z., Jelfs, K.E., Nitschke, J.R.. - In: JOURNAL OF THE AMERICAN CHEMICAL SOCIETY. - ISSN 0002-7863. - 143:24(2021), pp. 9009-9015. [10.1021/jacs.1c05172]

Availability:
This version is available at: 11583/2981653 since: 2023-09-05T10:13:50Z

Publisher:
American Chemical Society

Published
DOI:10.1021/jacs.1c05172

Terms of use:

This article is made available under terms and conditions as specified in the corresponding bibliographic description in the repository

Publisher copyright

(Article begins on next page)

15 October 2026

JACS
JOURNAL OF THE AMERICAN CHEMICAL SOCIETY
pubs.acs.org/JACS
Communication

Sterics and Hydrogen Bonding Control Stereochemistry and Self-Sorting in BINOL-Based Assemblies

You-Quan Zou,[†] Dawei Zhang,[†] Tanya K. Ronson, Andrew Tarzia, Zifei Lu, Kim E. Jelfs,* and Jonathan R. Nitschke*

Cite This: *J. Am. Chem. Soc.* 2021, 143, 9009–9015
Read Online
ACCESS | Metrics & More | Article Recommendations | Supporting Information

ABSTRACT: Here we demonstrate how the hydrogen-bonding ability of a BINOL-based dialdehyde subcomponent dictated the stereochemical outcome of its subsequent self-assembly into one diastereomeric helicate form when bearing free hydroxy groups, and another in the case of its methylated congener. The presence of methyl groups also altered the self-sorting behavior when mixed with another, short linear dialdehyde subcomponent, switching the outcome of the system from narcissistic to integrative self-sorting. In all cases, the axial chirality of the BINOL building block also dictated helicate metal center handedness during stereospecific self-assembly. A new family of stereochemically pure heteroleptic helicates were thus prepared using the new knowledge gained. We also found that switching from Fe^{II} to Zn^{II}, or the incorporation of a longer linear ligand, favored heteroleptic structure formation.

Downloaded via POLITECNICO DI TORINO on September 7, 2023 at 09:30:58 (UTC).
See https://pubs.acs.org/sharingguidelines for options on how to legitimately share published articles.

Coordination-driven self-assembly enables the rapid and efficient construction of intricate and functional architectures,[1,2] which have found an increasing number of uses.[3−5] Studies of the propagation of stereochemical information within supramolecular assemblies[6] have not only helped to elucidate possible origins of biological homochirality, but also opened new opportunities for chiral sensing and asymmetric transformation.[7] Enantiopure ligands have been used successfully to control the chirality of assemblies, whereby fixed ligand stereocenters dictate the stereochemical configurations of metal centers, and thus the overall chirality of an assembly.[8] A deeper understanding of the interplay between stereochemical elements during complex self-assembly processes allows the construction of increasingly complex structures with greater control over their stereochemistry.

Heteroleptic assemblies may result when ligands are designed to specifically match with other ligands within a multicomponent mixture.[9] Just as biological systems exhibit this phenomenon, self-sorting is prevalent in supramolecular chemistry.[10,11] Two self-sorting modes, narcissistic self-sorting[12] and integrative self-sorting,[13] are used to describe the extreme cases, which respectively give rise to homoleptic and heteroleptic architectures.[14] Designing systems to undergo integrative self-sorting remains a major challenge, and switching self-sorting behavior between the two modes in a controllable manner is of great interest.

In this work, we demonstrate how the methylation of a subcomponent built around the 1,1′-bi-2-naphthol (BINOL)[15] moiety alters the stereochemical outcome of subcomponent self-assembly (Figure 1).[16,17] Methylation also changed the course of self-assembly within a system containing both a BINOL-based subcomponent and a linear bis(formyl)pyridine from narcissistic to integrative self-sorting. Integrative self-sorting within this system enabled the stereoselective construction of a new family of enantiopure heteroleptic helicates.

Axially chiral subcomponents **A** (R = OH) and **B** (R = OMe) (Figure 1) were prepared in enantiopure form from commercially available (*R*)-BINOL as described in the Supporting Information (SI), sections 2.1 and 2.2. The reaction of **A** or **B** (3 equiv) with iron(II) bis(trifluoromethanesulfonyl)imide ($Fe(NTf_2)_2$, 2 equiv) and aniline (6 equiv) in acetonitrile at 70 °C produced enantiopure helicates Fe-**1** and Fe-**2**, respectively (Figure 1a). The ^{1}H NMR spectrum of Fe-**1** displayed only one set of ligand signals (Figures 1b and S16), consistent with the formation of a helicate with D_3 symmetry, where both iron(II) centers adopted the same Λ or Δ handedness.

In contrast, the ^{1}H NMR spectrum of Fe-**2**, prepared from methylated **B**, exhibited two distinct ligand environments, as reflected in the presence of two imine peaks (Figures 1b and S68). This spectrum is consistent with the formation of an Fe_2L_3 helicate with overall C_3 symmetry, having metal vertices of opposite handedness. Analogous assemblies formed from subcomponents **A** and **B** when $Zn(NTf_2)_2$ or $Co(NTf_2)_2$ were used in place of the iron(II) salt, resulting in helicates Zn-**1**, Zn-**2**, Co-**1**, and Co-**2** with ^{1}H NMR spectral features similar to those of Fe-**1** and Fe-**2** (Figures S9, S23, S59, and S77).

Following slow diffusion of diethyl ether into solutions of Zn-**1**, Co-**1**, and Co-**2** in acetonitrile, crystals suitable for X-ray diffraction were obtained. As shown in Figure 2a,b, both metal centers in Zn-**1** and Co-**1** adopted the same Λ handedness. However, opposite configurations (Λ and Δ) were observed for the two metal centers of helicate Co-**2** (Figure 2c). These

Received: May 19, 2021
Published: June 14, 2021

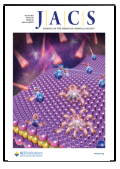

ACS Publications
© 2021 The Authors. Published by American Chemical Society

https://doi.org/10.1021/jacs.1c05172
J. Am. Chem. Soc. 2021, 143, 9009−9015

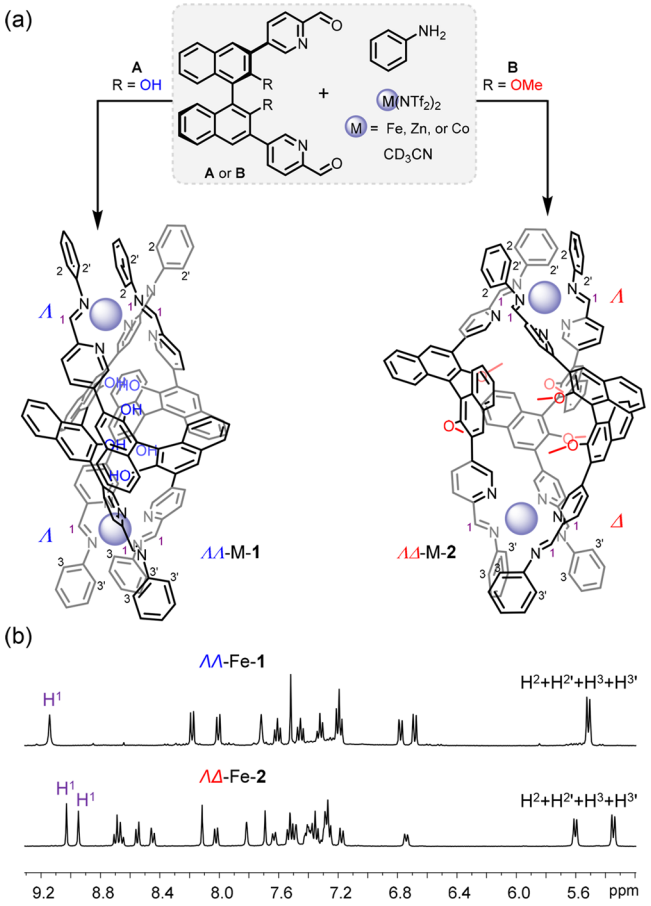

Figure 1. (a) Subcomponent self-assembly of **A** (R = OH) and **B** (R = OMe) with aniline and Co^{II}, Zn^{II}, or Fe^{II} afforded enantiopure helicates ΛΛ-M-**1** and ΛΔ-M-**2**, respectively. (b) ^{1}H NMR spectra of ΛΛ-Fe-**1** and ΛΔ-Fe-**2**. The imine protons (H^1) and *ortho*-protons of the aniline moieties (H^2, $H^{2'}$, H^3, $H^{3'}$) are indicated by purple and black labels, respectively.

solid-state observations are consistent with the results obtained from the solution NMR spectra described above.

The crystal structures help to explain how the presence or absence of methyl groups directed the outcome of self-assembly. Comparison of the structures of ΛΛ-Co-**1** and ΛΔ-Co-**2** (Figure 2b, 2c) reveals structure **1** to be more enclosed than its methylated congener, with aromatic stacking interactions between neighboring ligands (3.6−4.0 Å). Each of the three equatorial −OH groups form intramolecular hydrogen bonds (O···O distance 2.9−3.1 Å), stabilizing the configuration of the helicate. The bulkier methoxy groups in **B** force the helicates to adopt a *pseudo*-meso conformation. This configuration has a more open center to accommodate its six methoxy groups (Figure 2c). A comparison of the relative density functional theory (DFT)-calculated energies of the ΛΛ and ΛΔ structures for the Zn-**1** and Zn-**2** assemblies further supports these findings (SI, section 6). The ΛΛ assembly is more stable by 8.7 kJ mol^{-1} for Zn-**1**, while the ΛΔ assembly is more stable by 20.4 kJ mol^{-1} for Zn-**2**.

The difference in methylation between **A** and **B** led to distinct self-sorting behavior in the presence of another linear subcomponent and metal salts. When **B** (2 equiv) was mixed with 6,6′-diformyl-3,3′-bipyridine **C** (1 equiv), $Fe(NTf_2)_2$ (2 equiv), and aniline (6 equiv) in acetonitrile, heteroleptic helicate Fe-**4** was formed cleanly (Figure 3a, bottom). Fe-**4** contains two residues of **B** and one of **C**, as indicated by its ^{1}H NMR (Figure S80) and ESI-MS spectra (Figure S88), indicating that a thermodynamically favored integrative self-sorting process occurred. Trace amounts of homoleptic Fe-**2** were observed initially during self-assembly, which converted to Fe-**4** upon heating (Figure S80).

The structure of Fe-**4** was unambiguously confirmed by X-ray diffraction. As shown in Figure 3b, the two iron(II) centers are bridged by two residues of **B** and one of **C**, each condensed into a diimine ligand with two anilines. Both Fe^{II} centers adopt the same Λ handedness, generating a structure with C_2 symmetry. The metal centers are separated by 9.7280(8) Å, significantly shorter than the Co···Co distance of 13.351(1) Å in homoleptic Co-**2** but only slightly greater than the Fe···Fe distance of ca. 9.5 Å previously observed for Fe-**3**, which assembled from subcomponent **C** with aniline and Fe^{II}.[18]

Fe-**4** is the first member of a new class of heteroleptic helicates, consisting of two bent ligands and one linear ligand. We infer that the avoidance of steric eclipsing between the methoxy groups in homoleptic **2** (Figure 2c) drives the integrative self-sorting process, leading to **4**.

Narcissistic self-sorting was observed for the mixture of **A**, **C**, iron(II) triflimide, and aniline (Figure 3a, top), in contrast to the situation involving **B** and **C** described above. The products

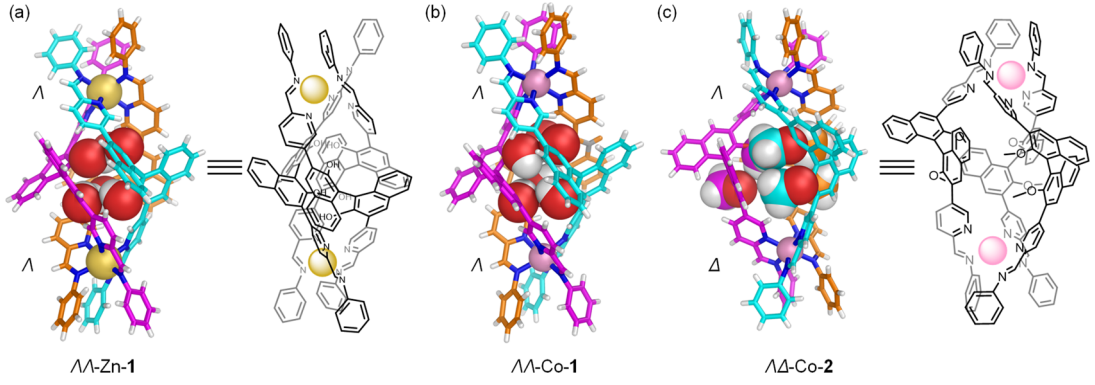

Figure 2. Crystal structures of (a) ΛΛ-Zn-**1**, (b) ΛΛ-Co-**1**, and (c) ΛΔ-Co-**2**. Hydroxy and methoxy groups are shown in space-filling mode, N is blue, H is white, and the carbon atoms of each independent ligand are drawn in fuchsia, cyan, and orange. Counteranions, disorder, and solvent of crystallization are omitted for clarity. [X-ray data for ΛΛ-Zn-**1**, ΛΛ-Co-**1**, and ΛΔ-Co-**2** are deposited as CCDC 2060204, 2060201, and 2060202, respectively.]

https://doi.org/10.1021/jacs.1c05172
J. Am. Chem. Soc. 2021, 143, 9009−9015

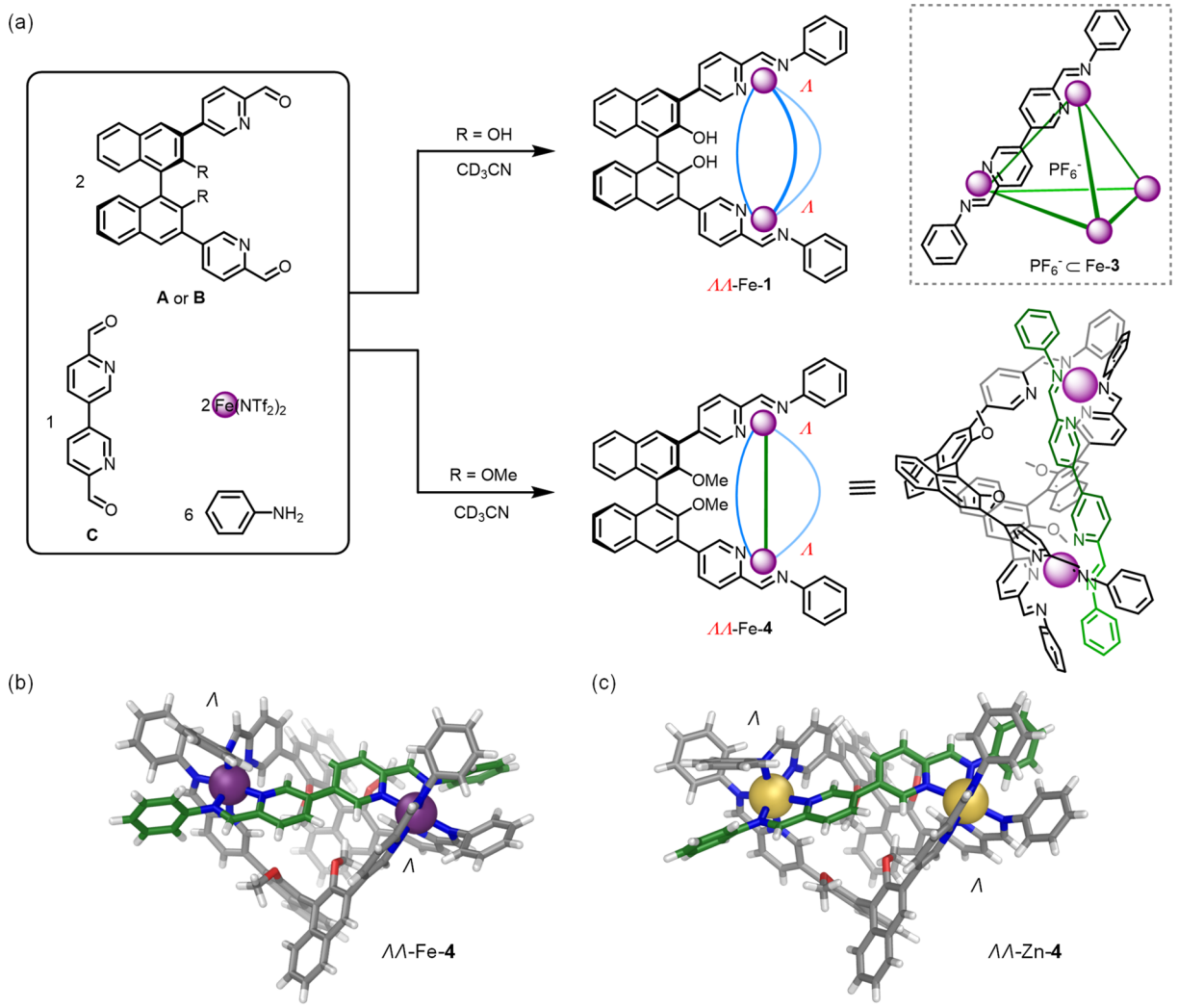

Figure 3. (a) Substituent effects on ligand self-sorting behavior. Bent **A** underwent narcissistic self-sorting with linear **C** (top), resulting in the simultaneous formation of Fe-**1** and Fe-**3**. Methylated **B**, in contrast, underwent integrative self-sorting with **C** (bottom). Crystal structures of (b) ΛΛ-Fe-**4** and (c) ΛΛ-Zn-**4**. Counteranions, disorder, and solvent molecules are omitted for clarity. [X-ray data for ΛΛ-Fe-**4** and ΛΛ-Zn-**4** are deposited as CCDC 2060203 and 2060205, respectively.]

of this reaction were homoleptic helicate ΛΛ-Fe-**1** and tetrahedron Fe-**3** (SI, section 3.2.1).[18,19]

Intriguingly, ^{1}H NMR peaks corresponding to heteroleptic Fe-**5**, an analog of Fe-**4** that incorporated two **A** residues and one **C**, were also observed after heating at 70 °C for 1 h, but these gradually disappeared in favor of peaks corresponding to homoleptic Fe-**1** (Figure S24). We were able to obtain metastable Fe-**5** in pure form by conducting the reaction at room temperature (SI, section 3.2.1). Its CD spectrum indicated ΛΛ stereochemistry of the two Fe^{II} centers (Figure S33), as with heteroleptic Fe-**4**.

We hypothesize that a driving force for the thermodynamically favored narcissistic self-sorting synthesis of Fe-**1** is the hydrogen-bonding interactions among the six −OH groups in ΛΛ-Fe-**1**, which stabilize the homoleptic structure.

Self-sorting outcomes were also found to be strongly affected by the identity of the metal salt and the length of the linear ligand. When Zn^{II} was used in place of Fe^{II}, both **A** and **B** underwent integrative self-sorting, giving rise to heteroleptic helicates as the thermodynamically favored products (SI, sections 3.2.2 and 4.2.2). The structure of ΛΛ-Zn-**4**, prepared from **B** and **C**, was further confirmed by X-ray crystallography (Figure 3c).

The integrative self-sorting behavior displayed by Zn^{II} may be driven by the inability of Zn^{II} and **C** to form a stable homoleptic structure in the absence of anion templates.[20] The more flexible coordination sphere of the larger Zn^{II} centers[21] may be better able to disperse the strain arising from differences in the preferred metal−metal distances of the two ligands, compared to the more rigid Fe^{II}, compensating for the stabilizing hydrogen-bonding interactions in homoleptic ΛΛ-Zn-**1** (Figure 2a).

When longer linear subcomponent **D** (Figure 4a) was used instead of **C** together with either **A** or **B**, $Fe(NTf_2)_2$, and aniline in acetonitrile, the heteroleptic helicates Fe-**6** and Fe-**7** (SI, sections 3.2.3 and 4.2.3) were formed via integrative self-sorting, along with the generation of the previously reported[22] homoleptic $Fe_4L^D_6$ assembly from **D** as a minor product (Figures 4a, S46, and S99). CD spectra of Fe-**6** and Fe-**7** were consistent with Δ handedness of the metal vertices for both complexes (Figures S55 and S108). Structures of the ΔΔ and ΛΛ assemblies of Fe-**6** and Fe-**7** were modeled using DFT (SI, section 6 describes the DFT methodology; Figures 4b,c and

https://doi.org/10.1021/jacs.1c05172
J. Am. Chem. Soc. 2021, 143, 9009−9015

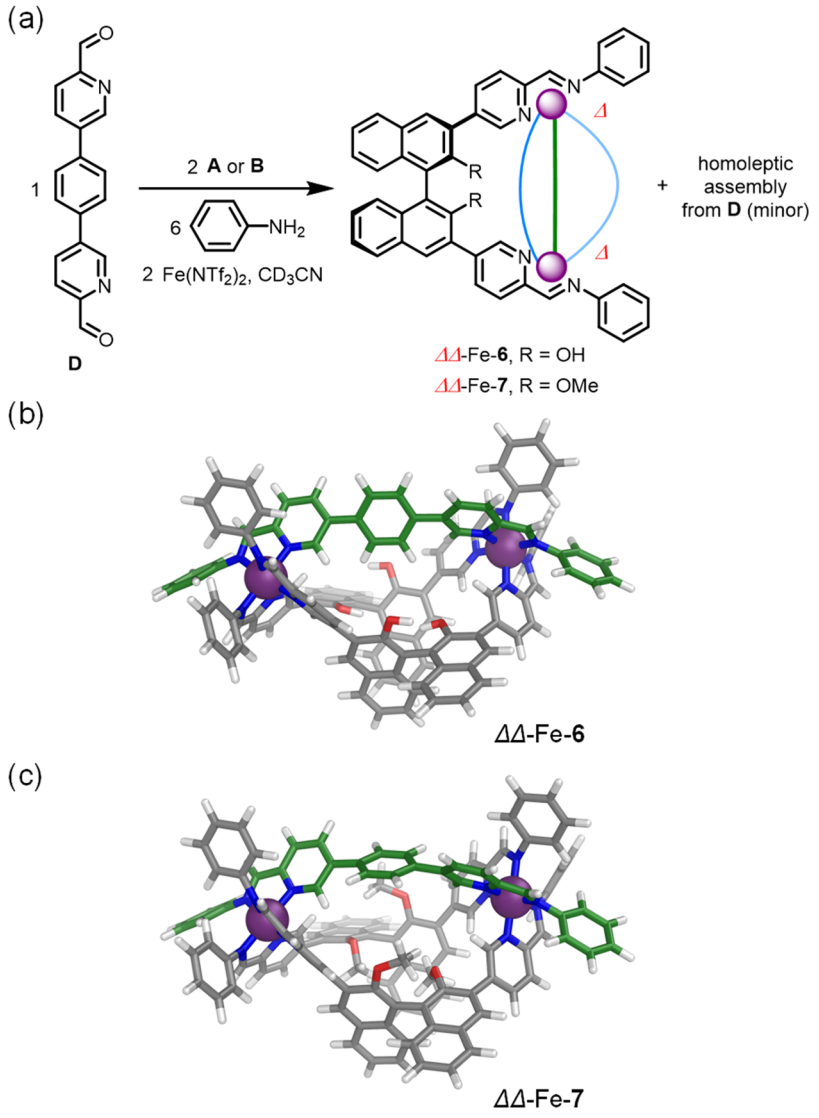

Figure 4. (a) Subcomponent self-assembly of **A** or **B** with longer **D**, aniline, and $Fe(NTf_2)_2$ generated the heteroleptic helicates ΔΔ-Fe-**6** and ΔΔ-Fe-7. DFT (PBE0/def2-SVP/D4)-optimized molecular models of (b) ΔΔ-Fe-**6** and (c) ΔΔ-Fe-7.

S121), providing $Fe^{II}\cdots Fe^{II}$ distances of 12.4 Å (Fe-**6**) and 12.3 Å (Fe-7), respectively, significantly longer than the metal−metal distance in Fe-**4** (9.7280(8) Å, Figure 3b). Similar results were obtained with $Zn(NTf_2)_2$ (SI, sections 3.2.4 and 4.2.4).

We hypothesize that the longer length of **D** as opposed to **C** brought the methoxy groups of **B** out of steric clash with each other as **B** scissored apart during heteroleptic self-assembly. This expansion of **B** thus enabled it to match the longer preferred distance between binding sites of **D**, whereas these methoxy groups eclipsed each other during heteroleptic assembly with shorter **C**. Relative DFT energies show that the ΛΛ assembly is more stable by 47.6 kJ mol^{-1} for Fe-**4**, while the ΔΔ structures are more stable by 63.8 and 16.3 kJ mol^{-1} for Fe-**6** and Fe-7, respectively (see SI, section 6 for details).

The self-assembly rules uncovered here provide new means of directing the formation of heteroleptic assemblies with controlled chirality. The new assemblies reported herein expose functionality—methoxy or hydroxyl groups—to their chirotopic interiors.[22] The inward orientation of such groups around a well-defined volume has been demonstrated to achieve reactivity modulation. Structures such as **1** and **2** may also be seen as a new class of enantiopure supramolecular receptor, which may be capable of binding cations tightly and selectively if their central cavities are shielded from the cations that knit the structures together.

■ ASSOCIATED CONTENT

Supporting Information

The Supporting Information is available free of charge at https://pubs.acs.org/doi/10.1021/jacs.1c05172.

Experimental and spectroscopic details, including Figures S1−S121 and Tables S1−S3 (PDF)

Accession Codes

CCDC 2060201−2060205 contain the supplementary crystallographic data for this paper. These data can be obtained free of charge via www.ccdc.cam.ac.uk/data_request/cif, or by emailing data_request@ccdc.cam.ac.uk, or by contacting The Cambridge Crystallographic Data Centre, 12 Union Road, Cambridge CB2 1EZ, UK; fax: +44 1223 336033.

https://doi.org/10.1021/jacs.1c05172
J. Am. Chem. Soc. 2021, 143, 9009−9015

AUTHOR INFORMATION

Corresponding Authors

Jonathan R. Nitschke − *Department of Chemistry, University of Cambridge, Cambridge CB2 1EW, United Kingdom*; Email: jrn34@cam.ac.uk

Kim E. Jelfs − *Department of Chemistry, Molecular Sciences Research Hub, White City Campus, Imperial College London, London W12 0BZ, United Kingdom*; orcid.org/0000-0001-7683-7630; Email: k.jelfs@imperial.ac.uk

Authors

You-Quan Zou − *Department of Chemistry, University of Cambridge, Cambridge CB2 1EW, United Kingdom*; orcid.org/0000-0002-3580-2295

Dawei Zhang − *Department of Chemistry, University of Cambridge, Cambridge CB2 1EW, United Kingdom*; orcid.org/0000-0002-0898-9795

Tanya K. Ronson − *Department of Chemistry, University of Cambridge, Cambridge CB2 1EW, United Kingdom*; orcid.org/0000-0002-6917-3685

Andrew Tarzia − *Department of Chemistry, Molecular Sciences Research Hub, White City Campus, Imperial College London, London W12 0BZ, United Kingdom*; orcid.org/0000-0001-8797-8666

Zifei Lu − *Department of Chemistry, University of Cambridge, Cambridge CB2 1EW, United Kingdom*

Complete contact information is available at: https://pubs.acs.org/10.1021/jacs.1c05172

Author Contributions

†Y.-Q.Z. and D.Z. contributed equally to this work.

Notes

The authors declare no competing financial interest.

ACKNOWLEDGMENTS

This work was supported by the European Research Council (695009) and the UK Engineering and Physical Sciences Research Council (EPSRC EP/P027067/1). The authors thank the Department of Chemistry NMR facility, University of Cambridge, for performing some NMR experiments, and the Diamond Light Source (UK) for synchrotron beamtime on I19 (CY21497). Y.-Q.Z. thanks the Sustainability and Energy Research Initiative (SAERI) foundation at the Weizmann Institute of Science (Israel) for a research fellowship. D.Z. acknowledges a Herchel Smith Research Fellowship from the University of Cambridge. Z.L. thanks the Cambridge Trusts and the Chinese Scholarship Council for Ph.D. funding. K.E.J. thanks the Royal Society for a University Research Fellowship and a Royal Society Enhancement Award 2018, and the ERC through Agreement Number 758370 (ERC-StG-PE5-CoMMaD). This work used the ARCHER2 UK National Supercomputing Service (https://www.archer2.ac.uk) via the UK's HEC Materials Chemistry Consortium, which is funded by the EPSRC (EP/L000202, EP/R029431, EP/T022213).

REFERENCES

(1) (a) Ruben, M.; Rojo, J.; Romero-Salguero, F. J.; Uppadine, L. H.; Lehn, J.-M. Grid-Type Metal Ion Architectures: Functional Metallosupramolecular Arrays. *Angew. Chem., Int. Ed.* **2004**, *43*, 3644−3662. (b) Yoshizawa, M.; Klosterman, J. K.; Fujita, M. Functional Molecular Flasks: New Properties and Reactions within Discrete, Self-Assembled Hosts. *Angew. Chem., Int. Ed.* **2009**, *48*, 3418−3438. (c) Chakrabarty, R.; Mukherjee, P. S.; Stang, P. J. Supramolecular Coordination: Self-Assembly of Finite Two- and Three-Dimensional Ensembles. *Chem. Rev.* **2011**, *111*, 6810−6918. (d) Custelcean, R. Anion Encapsulation and Dynamics in Self-Assembled Coordination Cages. *Chem. Soc. Rev.* **2014**, *43*, 1813−1824. (e) Yoshizawa, M.; Klosterman, J. K. Molecular Architectures of Multi-Anthracene Assemblies. *Chem. Soc. Rev.* **2014**, *43*, 1885−1898.

(2) For organic cages, see: (a) Evans, J. D.; Sumby, C. J.; Doonan, C. J. Synthesis and Applications of Porous Organic Cages. *Chem. Lett.* **2015**, *44*, 582−588. (b) Jordan, J. H.; Gibb, B. C. Molecular Containers Assembled through the Hydrophobic Effect. *Chem. Soc. Rev.* **2015**, *44*, 547−585. (c) Zhang, Z.; Kim, D. S.; Lin, C.-Y.; Zhang, H.; Lammer, A. D.; Lynch, V. M.; Popov, I.; Miljanić, O. Š.; Anslyn, E. V.; Sessler, J. L. Expanded Porphyrin-Anion Supramolecular Assemblies: Environmentally Responsive Sensors for Organic Solvents and Anions. *J. Am. Chem. Soc.* **2015**, *137*, 7769−7774. (d) Hasell, T.; Cooper, A. I. Porous Organic Cages: Soluble, Modular and Molecular Pores. *Nat. Rev. Mater.* **2016**, *1*, 16053. (e) Diaz-Moscoso, A.; Ballester, P. Light-Responsive Molecular Containers. *Chem. Commun.* **2017**, *53*, 4635−4652. (f) Stoddart, J. F. Mechanically Interlocked Molecules (MIMs)-Molecular Shuttles, Switches, and Machines (Nobel Lecture). *Angew. Chem., Int. Ed.* **2017**, *56*, 11094−11125. (g) Cram, D. J. Molecular Container Compounds. *Nature* **1992**, *356*, 29−36. (h) Zhang, G.; Mastalerz, M. Organic Cage Compounds-from Shape-Persistency to Function. *Chem. Soc. Rev.* **2014**, *43*, 1934−1947. (i) Yu, G.; Jie, K.; Huang, F. Supramolecular Amphiphiles Based on Host−Guest Molecular Recognition Motifs. *Chem. Rev.* **2015**, *115*, 7240−7303. (j) Duan, H.; Li, Y.; Li, Q.; Wang, P.; Liu, X.; Cheng, L.; Yu, Y.; Cao, L. Host-Guest Recognition and Fluorescence of a Tetraphenylethene-Based Octacationic Cage. *Angew. Chem., Int. Ed.* **2020**, *59*, 10101−10110.

(3) (a) Roukala, J.; Zhu, J.; Giri, C.; Rissanen, K.; Lantto, P.; Telkki, V. V. Encapsulation of Xenon by a Self-Assembled Fe_4L_6 Metallosupramolecular Cage. *J. Am. Chem. Soc.* **2015**, *137*, 2464−2467. (b) Preston, D.; Lewis, J. E.; Crowley, J. D. Multicavity $[Pd_nL_4]^{2n+}$ Cages with Controlled Segregated Binding of Different Guests. *J. Am. Chem. Soc.* **2017**, *139*, 2379−2386. (c) Akine, S.; Matsumoto, T.; Nabeshima, T. Overcoming Statistical Complexity: Selective Coordination of Three Different Metal Ions to a Ligand with Three Different Coordination Sites. *Angew. Chem., Int. Ed.* **2016**, *55*, 960−964. (d) Chen, T.-H.; Popov, I.; Kaveevivitchai, W.; Chuang, Y.-C.; Chen, Y.-S.; Jacobson, A. J.; Miljanić, O. Š. Mesoporous Fluorinated Metal−Organic Frameworks with Exceptional Adsorption of Fluorocarbons and CFCs. *Angew. Chem., Int. Ed.* **2015**, *54*, 13902−13906. (e) Luo, D.; Wang, X.-Z.; Yang, C.; Zhou, X.-P.; Li, D. Self-Assembly of Chiral Metal−Organic Tetartoid. *J. Am. Chem. Soc.* **2018**, *140*, 118−121. (f) Akine, S.; Miyashita, M.; Nabeshima, T. A Metallo-molecular Cage That Can Close the Apertures with Coordination Bonds. *J. Am. Chem. Soc.* **2017**, *139*, 4631−4634. (g) Sakata, Y.; Tamiya, M.; Okada, M.; Akine, S. Switching of Recognition First and Reaction First Mechanisms in Host−Guest Binding Associated with Chemical Reactions. *J. Am. Chem. Soc.* **2019**, *141*, 15597−15604.

(4) (a) Garcia-Simon, C.; Garcia-Borras, M.; Gomez, L.; Parella, T.; Osuna, S.; Juanhuix, J.; Imaz, I.; Maspoch, D.; Costas, M.; Ribas, X. Sponge-Like Molecular Cage for Purification of Fullerenes. *Nat. Commun.* **2014**, *5*, 5557. (b) Kishi, N.; Akita, M.; Yoshizawa, M. Selective Host-Guest Interactions of a Transformable Coordination Capsule/Tube with Fullerenes. *Angew. Chem., Int. Ed.* **2014**, *53*, 3604−3607. (c) Zhang, W. Y.; Lin, Y. J.; Han, Y. F.; Jin, G. X. Facile Separation of Regioisomeric Compounds by a Heteronuclear Organometallic Capsule. *J. Am. Chem. Soc.* **2016**, *138*, 10700−10707. (d) Liu, T.; Liu, Y.; Xuan, W.; Cui, Y. Chiral Nanoscale Metal-Organic Tetrahedral Cages: Diastereoselective Self-Assembly and Enantioselective Separation. *Angew. Chem., Int. Ed.* **2010**, *49*, 4121−4124.

(5) (a) Mal, P.; Breiner, B.; Rissanen, K.; Nitschke, J. R. White Phosphorus Is Air-Stable within a Self-Assembled Tetrahedral Capsule. *Science* **2009**, *324*, 1697−1699. (b) Galan, A.; Ballester, P. Stabilization of Reactive Species by Supramolecular Encapsulation. *Chem. Soc. Rev.* **2016**, *45*, 1720−1737.

(6) (a) Hamilton, T. D.; MacGillivray, L. R. Enclosed Chiral Environments from Self-Assembled Metal−Organic Polyhedra. *Cryst. Growth Des.* **2004**, *4*, 419−430. (b) Seeber, G.; Tiedemann, B. E. F.; Raymond, K. N. Supramolecular Chirality in Coordination Chemistry. In *Supramolecular Chirality*; CregoCalama, M., Reinboudt, D. N., Eds.; Springer: Berlin, Heidelberg, 2006; Vol. *265*, pp 147−183.
(7) (a) Albrecht, M.; Isaak, E.; Baumert, M.; Gossen, V.; Raabe, G.; Frohlich, R. "Induced Fit" in Chiral Recognition: Epimerization Upon Dimerization in the Hierarchical Self-Assembly of Helicate-Type Titanium(IV) Complexes. *Angew. Chem., Int. Ed.* **2011**, *50*, 2850−2853. (b) Brown, C. J.; Bergman, R. G.; Raymond, K. N. Enantioselective Catalysis of the Aza-Cope Rearrangement by a Chiral Supramolecular Assembly. *J. Am. Chem. Soc.* **2009**, *131*, 17530−17531.
(8) (a) Brotin, T.; Guy, L.; Martinez, A.; Dutasta, J.-P. Enantiopure Supramolecular Cages: Synthesis and Chiral Recognition Properties. In *Differentiation of Enantiomers II*; Schurig, V., Ed.; Springer: Cham, 2013; pp 177−230. (b) Gidron, O.; Ebert, M.-O.; Trapp, N.; Diederich, F. Chiroptical Detection of Nonchromophoric, Achiral Guests by Enantiopure Alleno-Acetylenic Helicages. *Angew. Chem., Int. Ed.* **2014**, *53*, 13614−13618.
(9) Wu, A.; Isaacs, L. Self-Sorting: The Exception or the Rule? *J. Am. Chem. Soc.* **2003**, *125*, 4831−4835.
(10) (a) Safont-Sempere, M. M.; Fernandez, G.; Würthner, F. Self-Sorting Phenomena in Complex Supramolecular Systems. *Chem. Rev.* **2011**, *111*, 5784−5814. (b) Lal Saha, M.; Schmittel, M. Degree of Molecular Self-Sorting in Multicomponent Systems. *Org. Biomol. Chem.* **2012**, *10*, 4651−4684. (c) He, Z.; Jiang, W.; Schalley, C. A. Integrative Self-Sorting: A Versatile Strategy for the Construction of Complex Supramolecular Architecture. *Chem. Soc. Rev.* **2015**, *44*, 779−789.
(11) (a) Li, J.; Nowak, P.; Otto, S. Dynamic Combinatorial Libraries: From Exploring Molecular Recognition to Systems Chemistry. *J. Am. Chem. Soc.* **2013**, *135*, 9222−9239. (b) Black, S. P.; Sanders, J. K.; Stefankiewicz, A. R. Disulfide Exchange: Exposing Supramolecular Reactivity through Dynamic Covalent Chemistry. *Chem. Soc. Rev.* **2014**, *43*, 1861−1872. (c) Ji, Q.; Lirag, R. C.; Miljanic, O. S. Kinetically Controlled Phenomena in Dynamic Combinatorial Libraries. *Chem. Soc. Rev.* **2014**, *43*, 1873−1884. (d) Osowska, K.; Miljanić, O. Š. Oxidative Kinetic Self-Sorting of a Dynamic Imine Library. *J. Am. Chem. Soc.* **2011**, *133*, 724−727. (e) Osowska, K.; Miljanić, O. Š. Self-Sorting of Dynamic Imine Libraries during Distillation. *Angew. Chem., Int. Ed.* **2011**, *50*, 8345−8349. (f) Howlader, P.; Mukherjee, P. S. Face and Edge Directed Self-Assembly of Pd_{12} Tetrahedral Nano-Cages and Their Self-Sorting. *Chem. Sci.* **2016**, *7*, 5893−5899. (g) Samanta, D.; Mukherjee, P. S. Multicomponent Self-Sorting of A Pd_7 Molecular Boat and Its Use in Catalytic Knoevenagel Condensation. *Chem. Commun.* **2013**, *49*, 4307−4309. (h) Johnson, A. M.; Hooley, R. J. Steric Effects Control Self-Sorting in Self-Assembled Clusters. *Inorg. Chem.* **2011**, *50*, 4671−4673.
(12) (a) Acharyya, K.; Mukherjee, S.; Mukherjee, P. S. Molecular Marriage through Partner Preferences in Covalent Cage Formation and Cage-to-Cage Transformation. *J. Am. Chem. Soc.* **2013**, *135*, 554−557. (b) Beaudoin, D.; Rominger, F.; Mastalerz, M. Chiral Self-Sorting of [2 + 3] Salicylimine Cage Compounds. *Angew. Chem., Int. Ed.* **2017**, *56*, 1244−1248. (c) Zheng, K.; Wang, H.; Chow, H. F. Organogelating and Narcissistic Self-Sorting Behaviour of Non-Preorganized Oligoamides. *Chem. Sci.* **2019**, *10*, 4015−4024. (d) Gidron, O.; Jirásek, M.; Trapp, N.; Ebert, M.-O.; Zhang, X.; Diederich, F. Homochiral [2]Catenane and Bis[2]catenane from Alleno-Acetylenic Helicates - A Highly Selective Narcissistic Self-Sorting Process. *J. Am. Chem. Soc.* **2015**, *137*, 12502−12505.
(13) (a) Chen, B.; Holstein, J. J.; Horiuchi, S.; Hiller, W. G.; Clever, G. H. Pd(II) Coordination Sphere Engineering: Pyridine Cages, Quinoline Bowls, and Heteroleptic Pills Binding One or Two Fullerenes. *J. Am. Chem. Soc.* **2019**, *141*, 8907−8913. (b) Cirulli, M.; Kaur, A.; Lewis, J. E. M.; Zhang, Z.; Kitchen, J. A.; Goldup, S. M.; Roessler, M. M. Rotaxane-Based Transition Metal Complexes: Effect of the Mechanical Bond on Structure and Electronic Properties. *J. Am. Chem. Soc.* **2019**, *141*, 879−889. (c) Schmittel, M.; Saha, S. From Self-Sorting of Dynamic Metal−Ligand Motifs to (Supra)Molecular Machinery in Action. In *Supramolecular Chemistry*; van Eldik, R., Puchta, R., Eds.; Academic Press, 2018; Vol. *71*, pp 135−175.
(14) (a) Pullen, S.; Clever, G. H. Mixed-Ligand Metal-Organic Frameworks and Heteroleptic Coordination Cages as Multifunctional Scaffolds-A Comparison. *Acc. Chem. Res.* **2018**, *51*, 3052−3064. (b) Wu, K.; Zhang, B.; Drechsler, C.; Holstein, J. J.; Clever, G. H. Backbone-Bridging Promotes Diversity in Heteroleptic Cages. *Angew. Chem., Int. Ed.* **2021**, *60*, 6403−6407. (c) Bloch, W. M.; Holstein, J. J.; Hiller, W.; Clever, G. H. Morphological Control of Heteroleptic *cis*- and *trans*-$Pd_2L_2L'_2$ Cages. *Angew. Chem., Int. Ed.* **2017**, *56*, 8285−8289. (d) Bloch, W. M.; Abe, Y.; Holstein, J. J.; Wandtke, C. M.; Dittrich, B.; Clever, G. H. Geometric Complementarity in Assembly and Guest Recognition of a Bent Heteroleptic *cis*-$[Pd_2L^A_2L^B_2]$ Coordination Cage. *J. Am. Chem. Soc.* **2016**, *138*, 13750−13755. (e) Clever, G. H.; Punt, P. Cation-Anion Arrangement Patterns in Self-Assembled Pd_2L_4 and Pd_4L_8 Coordination Cages. *Acc. Chem. Res.* **2017**, *50*, 2233−2243. (f) Schulte, T. R.; Holstein, J. J.; Clever, G. H. Chiral Self-Discrimination and Guest Recognition in Helicene-Based Coordination Cages. *Angew. Chem., Int. Ed.* **2019**, *58*, 5562−5566. (g) Zhu, R.; Bloch, W. M.; Holstein, J. J.; Mandal, S.; Schäfer, L. V.; Clever, G. H. Donor-Site-Directed Rational Assembly of Heteroleptic *cis*-$[Pd_2L_2L'_2]$ Coordination Cages from Picolyl Ligands. *Chem. - Eur. J.* **2018**, *24*, 12976−12982. (h) Li, R.-J.; Tessarolo, J.; Lee, H.; Clever, G. H. Multi-stimuli Control over Assembly and Guest Binding in Metallo-supramolecular Hosts Based on Dithienylethene Photoswitches. *J. Am. Chem. Soc.* **2021**, *143*, 3865−3873. (i) Preston, D.; Barnsley, J. E.; Gordon, K. C.; Crowley, J. D. Controlled Formation of Heteroleptic $[Pd_2(L_a)_2(L_b)_2]^{4+}$ Cages. *J. Am. Chem. Soc.* **2016**, *138*, 10578−10585.
(15) (a) Gutz, C.; Hovorka, R.; Klein, C.; Jiang, Q. Q.; Bannwarth, C.; Engeser, M.; Schmuck, C.; Assenmacher, W.; Mader, W.; Topic, F.; Rissanen, K.; Grimme, S.; Lützen, A. Enantiomerically Pure $[M_6L_{12}]$ or $[M_{12}L_{24}]$ Polyhedra from Flexible Bis(Pyridine) Ligands. *Angew. Chem., Int. Ed.* **2014**, *53*, 1693−1698. (b) Gutz, C.; Hovorka, R.; Schnakenburg, G.; Lützen, A. Homochiral Supramolecular M_2L_4 Cages by High-Fidelity Self-Sorting of Chiral Ligands. *Chem. - Eur. J.* **2013**, *19*, 10890−10894. (c) Klein, C.; Gutz, C.; Bogner, M.; Topic, F.; Rissanen, K.; Lützen, A. A New Structural Motif for an Enantiomerically Pure Metallosupramolecular Pd_4L_8 Aggregate by Anion Templating. *Angew. Chem., Int. Ed.* **2014**, *53*, 3739−3742. (d) Lützen, A.; Hapke, M.; Griep-Raming, J.; Haase, D.; Saak, W. Synthesis and Stereoselective Self-Assembly of Double- and Triple-Stranded Helicates. *Angew. Chem., Int. Ed.* **2002**, *41*, 2086−2089. (e) Stang, P. J.; Olenyuk, B. Directed Self-Assembly of Chiral, Optically Active Macrocyclic Tetranuclear Molecular Squares. *Angew. Chem., Int. Ed. Engl.* **1996**, *35*, 732−736. (f) Sun, B.; Nurttila, S. S.; Reek, J. N. H. Synthesis and Characterization of Self-Assembled Chiral $Fe^{II}_2L_3$ Cages. *Chem. - Eur. J.* **2018**, *24*, 14693−14700. (g) Tateishi, T.; Kojima, T.; Hiraoka, S. Chiral Self-Sorting Process in the Self-Assembly of Homochiral Coordination Cages from Axially Chiral Ligands. *Commun. Chem.* **2018**, *1*, 20. (h) Ye, Y.; Cook, T. R.; Wang, S. P.; Wu, J.; Li, S.; Stang, P. J. Self-Assembly of Chiral Metallacycles and Metallacages from a Directionally Adaptable Binol-Derived Donor. *J. Am. Chem. Soc.* **2015**, *137*, 11896−11899. (i) Jiao, J.; Dong, J.; Li, Y.; Cui, Y. Fine-Tuning of Chiral Microenvironments within Triple-Stranded Helicates for Enhanced Enantioselectivity. *Angew. Chem., Int. Ed.* **2021**, DOI: 10.1002/anie.202104111.
(16) (a) Yi, S.; Brega, V.; Captain, B.; Kaifer, A. E. Sulfate-Templated Self-Assembly of New M_4L_6 Tetrahedral Metal Organic Cages. *Chem. Commun.* **2012**, *48*, 10295−10297. (b) Sham, K. C.; Yiu, S. M.; Kwong, H. L. Dodecanuclear Hexagonal-Prismatic $M_{12}L_{18}$ Coordination Cages by Subcomponent Self-Assembly. *Inorg. Chem.* **2013**, *52*, 5648−5650. (c) Ferguson, A.; Staniland, R. W.; Fitchett, C. M.; Squire, M. A.; Williamson, B. E.; Kruger, P. E. Variation of Guest Selectivity within $[Fe_4L_4]^{8+}$ Tetrahedral Cages through Subtle Modification of the Face-Capping Ligand. *Dalton Trans.* **2014**, *43*,

https://doi.org/10.1021/jacs.1c05172
J. Am. Chem. Soc. 2021, 143, 9009−9015

14550−14553. (d) Lewing, D.; Koppetz, H.; Hahn, F. E. Reversible Formation and Transmetalation of Schiff-Base Complexes in Subcomponent Self-Assembly Reactions. *Inorg. Chem.* **2015**, *54*, 7653−7659. (e) Luo, D.; Zhou, X. P.; Li, D. Solvothermal Subcomponent Self-Assembly of Cubic Metal-Imidazolate Cages and Their Coordination Polymers. *Inorg. Chem.* **2015**, *54*, 10822−10828. (f) Yang, L.; Jing, X.; He, C.; Chang, Z.; Duan, C. Redox-Active M_8L_6 Cubic Hosts with Tetraphenylethylene Faces Encapsulate Organic Dyes for Light-Driven H_2 Production. *Chem. - Eur. J.* **2016**, *22*, 18107−18114.

(17) (a) Zhang, D.; Ronson, T. K.; Nitschke, J. R. Functional Capsules Via Subcomponent Self-Assembly. *Acc. Chem. Res.* **2018**, *51*, 2423−2436. (b) Young, M. C.; Holloway, L. R.; Johnson, A. M.; Hooley, R. J. A Supramolecular Sorting Hat: Stereocontrol in Metal-Ligand Self-Assembly by Complementary Hydrogen Bonding. *Angew. Chem., Int. Ed.* **2014**, *53*, 9832−9836. (c) Young, M. C.; Johnson, A. M.; Hooley, R. J. Self-promoted Post-synthetic Modification of Metal−ligand M_2L_3 Mesocates. *Chem. Commun.* **2014**, *50*, 1378−1380. (d) Young, M. C.; Johnson, A. M.; Gamboa, A. S.; Hooley, R. J. Achiral Endohedral Functionality Provides Stereochemical Control in Fe(II)-based Self-assemblies. *Chem. Commun.* **2013**, *49*, 1627−1629.

(18) Hristova, Y. R.; Smulders, M. M. J.; Clegg, J. K.; Breiner, B.; Nitschke, J. R. Selective Anion Binding by a "Chameleon" Capsule with a Dynamically Reconfigurable Exterior. *Chem. Sci.* **2011**, *2*, 638−641.

(19) von Krbek, L. K. S.; Roberts, D. A.; Pilgrim, B. S.; Schalley, C. A.; Nitschke, J. R. Multivalent Crown Ether Receptors Enable Allosteric Regulation of Anion Exchange in an Fe_4L_6 Tetrahedron. *Angew. Chem., Int. Ed.* **2018**, *57*, 14121−14124.

(20) Riddell, I. A.; Hristova, Y. R.; Clegg, J. K.; Wood, C. S.; Breiner, B.; Nitschke, J. R. Five Discrete Multinuclear Metal-Organic Assemblies from One Ligand: Deciphering the Effects of Different Templates. *J. Am. Chem. Soc.* **2013**, *135*, 2723−2733.

(21) Shannon, R. D. Revised Effective Ionic Radii and Systematic Studies of Interatomic Distances in Halides and Chalcogenides. *Acta Crystallogr., Sect. A: Cryst. Phys., Diffr., Theor. Gen. Crystallogr.* **1976**, *32*, 751−767.

(22) Ma, S.; Smulders, M. M. J.; Hristova, Y. R.; Clegg, J. K.; Ronson, T. K.; Zarra, S.; Nitschke, J. R. Chain-Reaction Anion Exchange between Metal−Organic Cages. *J. Am. Chem. Soc.* **2013**, *135*, 5678−5684.

https://doi.org/10.1021/jacs.1c05172
J. Am. Chem. Soc. 2021, 143, 9009−9015